



Contents lists available at ScienceDirect

Spectrochimica Acta Part A: Molecular and Biomolecular Spectroscopy

journal homepage: www.elsevier.com/locate/saa

Novel nanohybrids of cobalt(III) Schiff base complexes and clay: Synthesis and structural determinations



Ali Hossein Kianfar^{a,*}, Wan Ahmad Kamil Mahmood^b, Mohammad Dinari^a, Mohammad Hossein Azarian^b, Fatemeh Zare Khafri^c

^a Department of Chemistry, Isfahan University of Technology, Isfahan 84156-83111, Iran

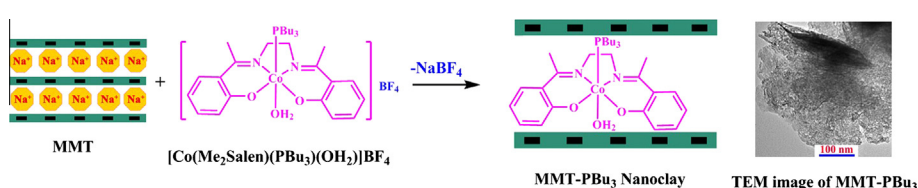
^b Department of Chemistry, Universiti Sains Malaysia, Penang, Malaysia

^c Department of Chemistry, College of Sciences Yasouj University, Yasouj, Iran

HIGHLIGHTS

- Novel cobalt Schiff base complexes were prepared and their structures were confirmed by different techniques.
- The X-ray crystallography results show that they are hexacoordinated in the solid state.
- Nanohybrid of the above complexes and MMT clay were prepared via ion-exchange method.
- FT-IR, TGA/DTG, XRD, SEM, EDX and TEM were used for the characterization of these materials.
- SEM and TEM show the resulting hybrid nanomaterials have layer structures.

GRAPHICAL ABSTRACT



ARTICLE INFO

Article history:

Received 1 December 2013

Received in revised form 1 February 2014

Accepted 19 February 2014

Available online 1 March 2014

Keywords:

X-ray crystallography

Cobalt Schiff base complexes

Cobalt(III) phosphine complexes

Insertion compounds

Modified clay

ABSTRACT

The $[\text{Co}(\text{Me}_2\text{Salen})(\text{PBu}_3)(\text{OH}_2)]\text{BF}_4$ and $[\text{Co}(\text{Me}_2\text{Salen})(\text{PPh}_3)(\text{Solvent})]\text{BF}_4$ complexes were synthesized and characterized by FT-IR, UV-Vis, ^1H NMR spectroscopy and elemental analysis techniques. The coordination geometry of $[\text{Co}(\text{Me}_2\text{Salen})(\text{PPh}_3)(\text{H}_2\text{O})]\text{BF}_4$ was determined by X-ray crystallography. It has been found that the complex is containing $[\text{Co}(\text{Me}_2\text{Salen})(\text{PPh}_3)(\text{H}_2\text{O})]\text{BF}_4$ and $[\text{Co}(\text{Me}_2\text{Salen})(\text{PPh}_3)(\text{EtOH})]\text{BF}_4$ hexacoordinate species in the solid state. Cobalt atom exhibits a distorted octahedral geometry and the Me_2Salen ligand has the N2O2 coordinated environment in the equatorial plane. The $[\text{Co}(\text{Me}_2\text{Salen})(\text{PPh}_3)(\text{H}_2\text{O})]\text{BF}_4$ complex shows a dimeric structure via hydrogen bonding between the phenolate oxygen and hydrogens of coordinated H_2O molecule. These complexes were incorporated into Montmorillonite-K10 nanoclay. The modified clays were identified by FT-IR, XRD, EDX, TGA/DTA, SEM and TEM techniques. According to the XRD results of the new nanohybrid materials, the Schiff base complexes are intercalated in the interlayer spaces of the clay. SEM and TEM micrographs show that the resulting hybrid nanomaterials have layer structures. Also, TGA/DTG results show that the intercalation reaction was taken place successfully.

© 2014 Published by Elsevier B.V.

* Corresponding author. Tel.: +98 311 391 3245; fax: +98 311 391 2350.

E-mail addresses: akianfar@cc.iut.ac.ir, asarvestani@yahoo.com (A.H. Kianfar).

Introduction

During the past few years, terms like nanomaterials, nanocomposites and nanosystems have become designer. In fact anything with 'nano' attached to it has nearly a magical effect – not so much on performance as on expectations. There exceptional size-dependent properties make these materials superior and indispensable as they show unusual physical, chemical and biological properties [1,2]. Along with the different nanomaterials, nanoclays compose a multitalented area of exploration [3–6]. Due to its large value of aspect ratio, diameters in nanometer range, and thermal resistance, clay minerals have many attentions in recent years [7]. Sodium Montmorillonite (MMT) is the most commonly used clay owing to its natural abundance, high aspect ratio and high cationic exchange capacity (about 80–120 meq/100 g) [8–10].

Cobalt Schiff base complexes have been studied extensively. They are investigated as models for the Cobalamine (B_{12}) coenzymes [11] classified as an oxygen carrier [12]. They applied as a catalyst for the preparative oxygenation of phenols [13] and amines [14]. Cobalt(III) salen catalytic activity has been investigated. The catalytically active species contains Co(III) oxidation state [15].

Cobalt(III) Schiff base complexes with formula of $[CoL(PR_3)(OH_2)]^+$ (where L = tetradentate N_2O_2 Schiff bases) show that these types of complexes are in equilibrium with phosphines and amines to form $[CoL(PR_3)_2]^+$ and $[CoL(PR_3)(amine)]^+$ [16–25], but there is not any information about their structure. So to extension the studies on the structure of these type of complexes, Me_2Salen (bis(2-hydroxyacetophenone)ethylenediamine) Schiff base was prepared by the condensation of 2-hydroxyacetophenone within 1,2-ethylenediamine. The tertiary phosphine cobalt(III) complexes of synthesized ligand were prepared in methanol solvent (Scheme 1). The prepared complexes were identified by FT-IR, 1H NMR, UV-Vis spectroscopy and elemental analysis. The coordination geometry of $[Co(Me_2Salen)(PPh_3)_2]BF_4$ was determined by X-ray crystallography. The synthesized complexes were incorporated into Montmorillonite K-10 nanoclay. The modified clay was identified and studied via FT-IR, XRD, TG/DTA, SEM, EDX and TEM.

Experimental

Materials

All of the chemicals and solvents used for synthesis were of commercially available reagent grade and they were used without purification. Montmorillonite K-10 (MMT) with cation-exchange capacity of 119 meq/100 g was provided by Aldrich.

Characterizations

Fourier transform infrared (FT-IR) spectra were recorded as KBr discs on a FT-IR JASCO-680 spectrophotometer in the 4000–400 cm^{-1} . The elemental analysis was determined on a CHN-O-Heraeus elemental analyzer. UV-Vis spectra were recorded on a JASCO V-570 spectrophotometer in the 190–900 nm. The 1H NMR spectra were recorded in $CDCl_3$ on DPX-400 MHz FT-NMR. The

X-ray single crystal structure analysis was obtained by using Bruker smart Apex II-2009 CCD area detector diffractometer. The X-ray diffraction (XRD) was recorded on high resolution X-Ray diffractometer system model PANalytical X'PRO MRD PW3040. Transmission electron microscopy (TEM) studies were performed using Zeiss Libra[®]120 TEM system. The thermal stability of specimens was tested using PERKIN ELMER TGA7 1991 thermogravimetric analyzer from ambient temperature to 900 °C at a heating rate of 20 °C/min under nitrogen gas. Scanning electron microscopy (SEM) was recorded on QUANTA FEG 650 2012 SEM system. Energy Dispersive X-ray Analysis (EDX) (EDAX Falcon System) was conducted to analyze the presence of elements in the specimens that have been sputtered with carbon black.

Synthesis of Schiff base ligands

The Schiff base ligand, H_2Me_2Salen , was prepared according to the literature [26] by condensation between 1,2-ethylenediamine and 2-hydroxyacetophenone (1:2 mole ratio) in methanol and recrystallized by dichloromethane/methanol mixed solvent through the partial evaporation of dichloromethane.

Synthesis of metal Schiff base complexes

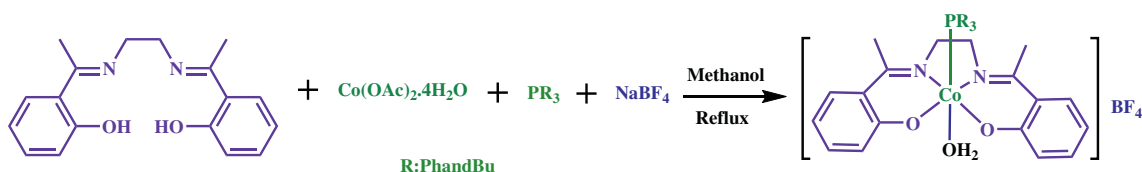
The general procedure for synthesis of $[Co(Me_2Salen)(PBu_3)(H_2O)]BF_4$, $[Co(Me_2Salen)(PPh_3)(H_2O)]BF_4$ complexes is as follows: an appropriate amount of cobalt(II)acetatetetrahydrate (0.249 g, 1.0 mmol), phosphine (1.0 mmol) were added to a methanolic solution (40 mL) of H_2Me_2Salen (0.296 g, 1.0 mmol). The reaction was refluxed for 1 h. The formed Co(II) complex was oxidized by blowing air into the solution for 2 h, then it was filtered. To the filtrate, an appropriate amount of sodium tetrafluoroborate (.110 g, 1.0 mmol) was added. The green crystals formed after 48 h. The crystals filtered off, washed with methanol and recrystallized from 2:1 ratio of methanol/ethanol and dried in vacuum at 65 °C.

$[Co(Me_2Salen)(PBu_3)(OH_2)]BF_4$ Yield (75%). Anal. calc. for $C_{30}H_{47}N_2O_3PF_4Co$: C, 60.89; H, 8.01; N, 4.73%. Found; C, 61.35; H, 8.12; N, 4.85%. FT-IR (KBr cm^{-1}) ν_{max} 2956, 2921, 2863 (C–H), 1597 (C=N), 1439 (C=C), 1085 (BF_4^-). 1H NMR ($CDCl_3$, δ , ppm): 0.70–0.80 (t, 9H, CH_3), 1.15–1.31 (m, 18H, CH_2), 2.70 (s, 6H, CH_3), 3.90–4.10 (d, 4H, CH_2), 6.59–7.67 (m, 8H, Aromatic). UV-Vis, λ_{max} (nm) (Ethanol): 636 (780), 397 (5700), 336 (5600).

$1/2[Co(Me_2Salen)(PPh_3)(CH_3CH_2OH)]BF_4 \cdot 1/2[Co(Me_2Salen)(PPh_3)(H_2O)]BF_4$ Yield (80%). Anal. calc. for $C_{37}H_{37}N_2O_3PF_4BCo$: C, 60.51; H, 5.08; N, 3.81%. Found; C, 61.44; H, 5.17; N, 3.83%. FT-IR (KBr cm^{-1}) ν_{max} 3058 (C–H), 1592 (C=N), 1438 (C=C), 1086 (BF_4^-). 1H NMR ($CDCl_3$, δ , ppm): 2.30 (s, 3H, CH_3 , ethanol), 2.70 (s, 6H, CH_3), 3.50–4.30 (m, 6H, CH_2 , ethanol and bridge ethylene), 6.42–7.52 (m, 23H, Aromatic). UV-Vis, λ_{max} (nm) (Ethanol): 724 (1100), 405 (5700), 337 (10,000).

Synthesis of intercalation compounds

The 0.75 g of MMT was added to an ethanol solution containing $[Co(Me_2Salen)(PBu_3)(H_2O)]BF_4$ or $[Co(Me_2Salen)(PPh_3)(H_2O)]BF_4$ (0.075 g) complexes. The reaction mixture was refluxed for 24 h



Scheme 1. The structure of Schiff base and its complexes.

and was filtered off. The green precipitate was washed with ethanol, methanol and acetone for several times, and then it was dried at 65 °C.

MMT white, FT-IR (KBr cm^{-1}) ν_{max} 2750–3600 (H_2O), 1645 (OH), 900–1300 (Si–O), 527 (Al–O) and 462 (Mg–O).

MMT-[Co(Me₂Salen)(PBU₃)(H₂O)] (MMT-PBU₃): color: green, FT-IR (KBr cm^{-1}) ν_{max} 2750–3600 (H_2O), 2959, 2933, 2873 (C–H), 1631 (OH), 1592 (C=N), 1440 (C=C), 900–1300 (Si–O), 524 (Al–O) and 470 (Mg–O).

MMT-[Co(Me₂Salen)(PPh₃)(H₂O)] (MMT-PPh₃): color: green, FT-IR (KBr cm^{-1}) ν_{max} 2750–3600 (H_2O), 1631 (OH), 1598 (C=N), 1439 (C=C), 900–1300 (Si–O), 524 (Al–O) and 468 (Mg–O).

Crystal structure determination and refinement of [Co(Me₂Salen)(PPh₃)(H₂O)]BF₄

The X-ray diffraction measurements were made on a STOE IPDS-2T diffractometer with graphite monochromated Mo K α radiation.

For [Co(Me₂Salen)(PPh₃)(H₂O)]BF₄ complex green plate crystal with a dimension of 0.11 × 0.16 × 0.20 mm chosen and mounted on a glass fiber and used for data collection. Cell constants and an orientation matrix for data collection were obtained by least-squares refinement of diffraction data from 17,496 unique reflections. Data were collected at a temperature of 100(2) K to a maximum 2 θ value of 58.00° in a series of ω scans in 1° oscillations and integrated using the Stoe X-Area software package. The numerical absorption coefficient, μ , for Mo K α radiation is 0.710 mm^{-1} . A numerical absorption correction was applied using X-RED and X-SHAPE [27] software. The data were corrected for Lorentz and Polarizing effects. The structures were solved by direct methods [28] and subsequent difference Fourier maps and then refined on F^2 by a full-matrix least-squares procedure using anisotropic displacement parameters [29]. All of hydrogen atoms were located in a difference Fourier map and then refined isotropically. Atomic factors are from International Tables for X-ray Crystallography. All refinements were performed using the X-STEP32 crystallographic software package [30].

Table 1
Crystallographic and structure refinements data for [Co(Me₂Salen)(PPh)(Solvent)]BF₄.

Formula	C ₃₈ H ₃₉ CoN ₂ O ₃ P, C ₃₆ H ₃₅ CoN ₂ O ₃ P, 2(BF ₄)
Formula weight	1468.79
Temperature (K)	100(2)
Wavelength λ (Å)	0.71073
Crystal system	Monoclinic
Space group	$P2_1/c$
Crystal size (mm^3)	0.11 × 0.16 × 0.20
a (Å)	21.2201(4)
b (Å)	15.5368(3)
c (Å)	20.4774(4)
α	90.00
β (°)	102.554(1)
γ	90.00
Density (calc.) (g cm^{-3})	1.480
θ ranges for data collection	1.8–29.0
$F(000)$	3040
Absorption coefficient	0.633
Index ranges	–28 ≤ h ≤ 28 –21 ≤ k ≤ 21 –27 ≤ l ≤ 27
Data collected	128,093
Unique data (R_{int})	17496, (0.176)
Parameters, restraints	871, 0
Final R_1 , wR_2^a (obs. data)	0.0978, 0.1720
Final R_1 , wR_2^a (all data)	0.1658, 0.1722
Goodness of fit on F^2 (S)	1.09
Largest diff peak and hole (e Å^{-3})	0.86, –0.70

A summary of the crystal data, experimental details and refinement results are given in Table 1 for [Co(Me₂Salen)(PPh₃)(H₂O)]BF₄ complex. It is notable that, the asymmetric unit also contains solvent molecules, which could not be modeled. Therefore, the diffracted contribution of the solvent molecules was removed by the subroutine SQUEEZE in PLATON. It is notable that although the structure refined correctly for the complex but the high R_{int} (0.1759) and R value (0.0978) is due to cracking of the crystal.

Results and discussion

FT-IR characteristics

The FT-IR spectra of the cobalt(III) complexes exhibit several bands in the 400–4000 cm^{-1} region (Section ‘Characterizations’). The C=N bond vibrations appears in 1592 and 1597 cm^{-1} region for the synthesized complexes. These stretching are generally shifted to a lower frequency relative to the free Schiff base, indicating a decrease in the C=N bond order due to the coordinate bond formation between the metal and the imine nitrogen [31]. The C–H stretching of PBU₃ coordinated ligands were appeared in 2863, 2956 and 2921 cm^{-1} region. The stretching vibration of BF₄[–] counter ion appear at about 1058 and 1086 cm^{-1} for Co(Me₂Salen)(PBU₃)(OH₂)]BF₄, [Co(Me₂Salen)(PPh₃)(OH₂)]–BF₄, respectively.

The MMT shows some peaks related to its functional groups. A broad peak is seen in the range of 3600–2700 cm^{-1} that is related to the interlayer absorbed water molecules. A weak band is appeared at 1645 cm^{-1} which is related to the OH bending. The Si–O stretching peak is appeared in the range of 1300–900 cm^{-1} . The peaks at 462 and 527 cm^{-1} are related to Mg–O and Al–O, respectively (Fig. 1).

The FT-IR spectra of intercalation compounds (MMT-PBU₃ and MMT-PPh₃) show some changes relative to the pure MMT (Fig. 1). Some peaks that are related to the complexes were seen in the new intercalation compounds. The C=N band was appeared at about 1600 cm^{-1} . The CH vibrations of PBU₃ were seen in the range of 2959–2873 cm^{-1} and the C=C stretching was appeared at about 1440 cm^{-1} . These observations confirm the formation of the nanohybrid materials.

Electronic spectra

The spectral data of the synthesized complexes were listed in Section ‘Characterizations’. In both complexes, the band in the

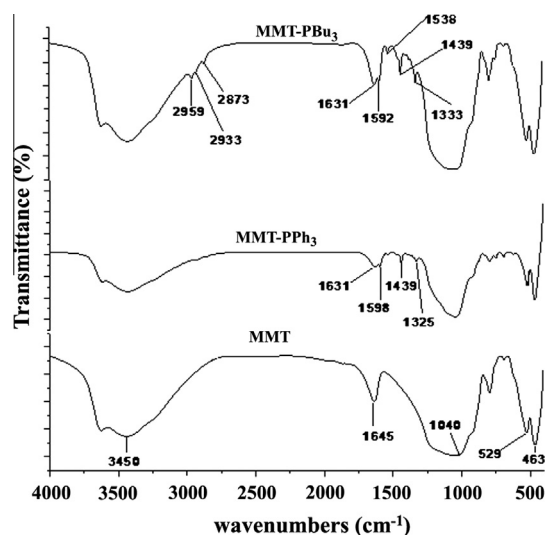


Fig. 1. The FT-IR spectra of the hybrid materials.

^a $R_1 = \sum ||F_o| - |F_c|| / \sum |F_o|$, $wR_2 = \left[\frac{\sum (w(F_o^2 - F_c^2))^2}{\sum w(F_o^2)} \right]^{1/2}$.

Table 2
Selected bond distances (Å) and bond angles (°) for [Co(Me₂Salen)(PPh₃)(EtOH)]BF₄.

Bond distances		Bond angles	
Co1–N1	1.910(4)	P1–Co1–N1	96.29(11)
Co1–N2	1.901(3)	P1–Co1–N2	96.28(11)
Co1–O1	1.871(3)	P1–Co1–O1	87.24(9)
Co1–O2	1.880(3)	P1–Co1–O2	88.55(9)
Co1–Ow	2.107(3)	P1–Co2–O1 WA	177.15(9)
Co1–P1	2.2222(12)	O1 WA–Co1–N1	85.74(14)
O1–C19	1.308(5)	O1 WA–Co1–N2	85.79(14)
O2–C34	1.319(5)	O1 WA–Co1–O1	90.64(13)
N1–C25	1.302(5)	O1 WA–Co1–O2	89.39(12)
N2–C28	1.295(5)	O1–Co1–N2	176.24(14)
N1–C26	1.476(5)	O2–Co1–N1	175.01(14)
N2–C27	1.477(5)	O1–Co1–O2	85.78(12)
O1W–H1W	0.8476	N1–Co1–N2	87.72(15)
		O1–Co1–N1	93.22(14)
		O2–Co1–N2	92.97(14)

Table 3
Selected bond distances (Å) and bond angles (°) for [Co(Me₂Salen)(PPh₃)(OH₂)]BF₄.

Bond distances		Bond angles	
Co1–N1	1.898(4)	P1–Co1–N1	94.84(11)
Co1–N2	1.909(3)	P1–Co1–N2	93.22(11)
Co1–O1	1.879(3)	P1–Co1–O1	91.87(9)
Co1–O2	1.867(3)	P1–Co1–O2	88.57(9)
Co1–Ow	2.102(3)	P1–Co2–O1W	175.85(9)
Co1–P1	2.2475(12)	O1WA–Co1–N1	89.30(13)
O1–C19	1.322(5)	O1WA–Co1–N2	87.12(13)
O2–C34	1.315(5)	O1WA–Co1–O1	87.74(12)
N1–C25	1.298(5)	O1WA–Co1–O2	87.29(12)
N2–C28	1.293(5)	O1–Co1–N2	174.84(14)
N1–C26	1.488(5)	O2–Co1–N1	176.27(14)
N2–C27	1.475(5)	O1–Co1–O2	85.45(13)
O1W–H1W	0.8476	N1–Co1–N2	87.47(15)
O1WB–H1WB	0.8503	O1–Co1–N1	92.90(14)
O1WB–H2WB	0.8535	O2–Co1–N2	93.87(13)
O1B–H2WB	2.020		

253–255 nm region, involves $\pi \rightarrow \pi^*$ transition related to aromatic ring. The band in the 304–307 nm region, involves $\pi \rightarrow \pi^*$ transition related to azomethine group. The cobalt(III) complexes show an absorption band related to charge transfer transition (LMCT) at about 395–412 nm region [16,32–38]. In addition, a $d-d$

transition was seen in the range of 600–750 nm for the complexes [18,19].

¹H NMR spectra

The chemical shift (δ , ppm) of different protons of the cobalt(III) complexes is presented in Section 'Characterizations'. The ¹H NMR of complexes is in line with the proposed structures. The hydrogens of the tributyl phosphine in the [Co(Me₂Salen)(PPh₃)(H₂O)]BF₄ were seen in the range of 0.70–1.31 ppm. The CH₃ of butyl was seen as triplet. The methylene groups were seen as multiplet. The hydrogens of methyl groups of CH₃ were seen as singlet. The CH₂ hydrogen of ethylene bridge were seen as doublet at about 3.58–3.92 ppm. The hydrogens of aromatic rings were seen in the range of 6.42–7.67 ppm. The complex of [Co(Me₂Salen)(PPh₃)(H₂O)]BF₄ shows some additional protons related to ethanol in 2.3 ppm and in the range of 3.50–4.30 ppm overlapped with ethylene bridge.

Description of the molecular structure of [Co(Me₂Salen)(PPh₃)(H₂O)]BF₄

The [Co(Me₂Salen)(PPh₃)(H₂O)]BF₄ complex was characterized by X-ray diffraction and crystallized in the Monoclinic space group

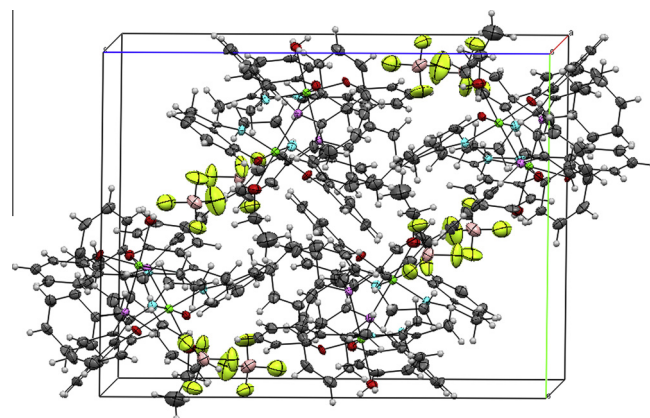


Fig. 3. Packing diagram of the unit cell of [Co(Me₂Salen)(PPh₃)(Solvent)]BF₄.

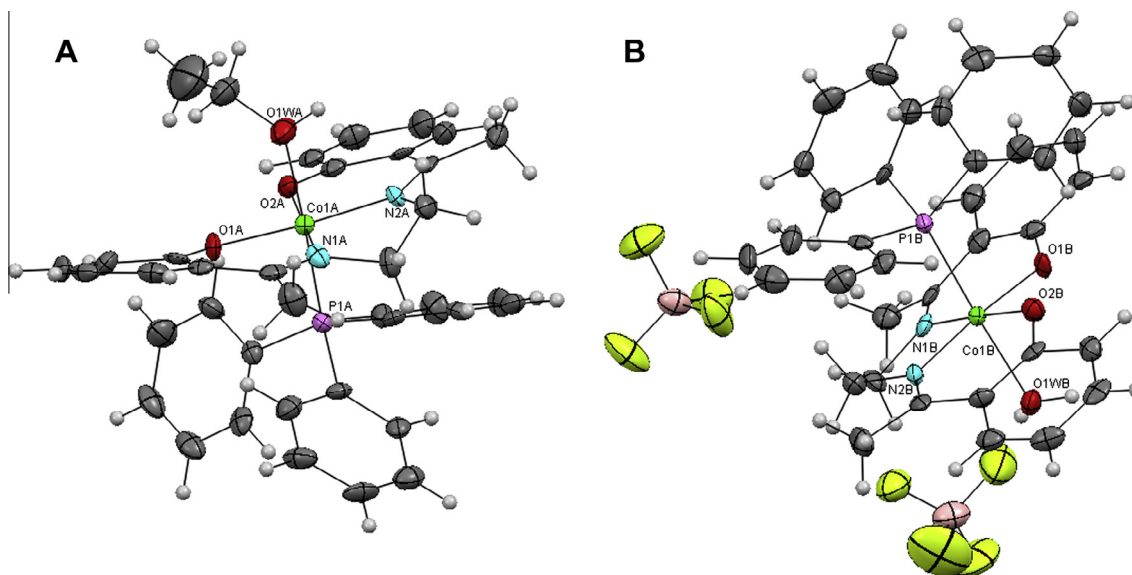


Fig. 2. The labeled diagram of [Co(Me₂Salen)(PPh₃)(EthOH)]BF₄(A) and [Co(Me₂Salen)(PPh₃)(OH₂)]BF₄(B).

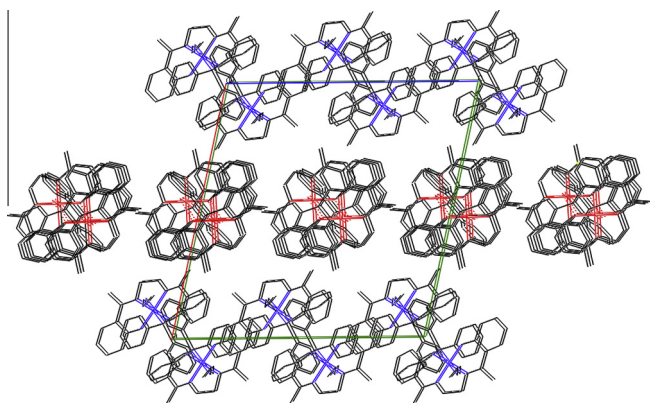


Fig. 4. A view of the extended network of complex $[\text{Co}(\text{Me}_2\text{Salen})(\text{PPh}_3)(\text{Solvent})]\text{BF}_4$ with the intermolecular hydrogen bonds (dashed red lines) between molecules B. (For interpretation of the references to color in this figure legend, the reader is referred to the web version of this article.)

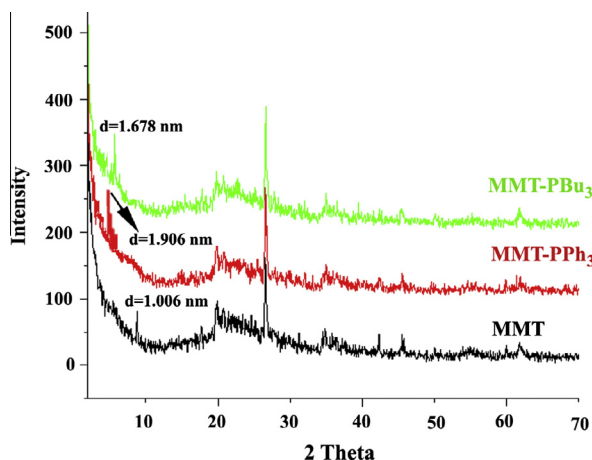


Fig. 5. The XRD patterns of the hybrid materials.

$P2_1/a$. X-ray diffraction data and selected bond lengths and angles are listed in Tables 1–3, respectively. The complex crystallizes with two independent molecules ($[\text{Co}(\text{Me}_2\text{Salen})(\text{PPh}_3)(\text{EtOH})]\text{BF}_4$ (A complex) and $[\text{Co}(\text{Me}_2\text{Salen})(\text{PPh}_3)(\text{H}_2\text{O})]\text{BF}_4$ (B complex)) in the asymmetric unit (Fig. 2). The packing diagram of the complex is shown in Fig. 3.

Each cobalt atom is coordinated in a distorted octahedral geometry, the Me_2Salen ligand has the N_2O_2 coordinated in the equatorial plane. $\text{P}-\text{Co}-\text{N}/\text{O}$ angles were distributed from $87.24(1)^\circ$ to

$96.29(2)^\circ$. The $\text{Co}-\text{N}_1$, $\text{Co}-\text{N}_2$, $\text{Co}-\text{O}_1$ and $\text{Co}-\text{O}_2$ distances of 1.910(4), 1.901(3), 1.871(3) and 1.880(3) Å and 1.898(4), 1.909(3), 1.879(3) and 1.867(3) Å for A and B complexes, respectively, are similar to those in N_2O_2 -salen cobalt complexes [39–41]. Interestingly the A and B complexes have a partial difference in their structures. As can be seen in Fig. 2, molecule A has an ethanol group in an axial position *trans* to the PPh_3 group while in B a water molecule occupies this position. The $\text{Co}-\text{O}$ distances (1.871(3), 1.880(3) N_2O_2 -salen cobalt Å for A and 1.879(3), 1.867(3) Å for B) are smaller than the $\text{Co}-\text{O}_w$ distances (2.107(3) Å (A) and 2.102(3) Å (B)), due to the greater *trans* influence of the P1 atom with respect to the N1 and N2 atoms. The $\text{Co}-\text{P}$ bond distances of apical positions are 2.222(1) and 2.247(1) for $\text{Co}-\text{P1A}$ and $\text{Co}-\text{P1B}$, respectively.

The extended network of complex is determined by intermolecular bonds (for example the hydrogen bonding between the coordinated phenolate oxygen and the coordinated water ($\text{O1B}-\text{H2WB} = 2.020$ Å)) in molecule B which leads to aggregation and to a supramolecular structure (Fig. 4).

All angles around the cobalt center deviate significantly from 90° indicating a regular distortion. For example in the complex A the ligand-cobalt-ligand bond angles in the equatorial plane consist of two angles that are larger than 90° ($\text{O1}-\text{Co1}-\text{N1}$) ($93.22(22)^\circ$), ($\text{O2}-\text{Co1}-\text{N2}$) ($92.97(22)^\circ$) and two smaller angles ($\text{O1}-\text{Co1}-\text{O2}$) ($85.87(2)^\circ$), ($\text{N1}-\text{Co1}-\text{N2}$) ($87.72(2)^\circ$) are similar to those in N_2O_2 -salen cobalt complexes [42]. Also the summations of these angles are nearly 360° and shows that the cobalt atom is in a square planer environment of N_2O_2 atoms.

X-ray diffraction

The XRD analysis confirmed that the intercalation reaction was successful with the cationic complexes. The MMT layers were propped apart upon swelling in ethanol and the basal distances became higher after the ion-exchange process by the cationic complexes compared to the original MMT, even after removing the solvent and washing off excess metal complexes from the outer surface of the clay. The d -spacing of unmodified MMT ($d = 1.006$ nm) is calculated from the peak position at $2\theta = 8.78^\circ$ using Bragg's equation. The diffraction peak of the $\text{MMT}-\text{PPh}_3$ and $\text{MMT}-\text{PBu}_3$ nanohybrids shifts to a new position at $2\theta = 4.63^\circ$ ($d = 1.906$ nm) and at $2\theta = 5.26^\circ$ ($d = 1.678$ nm) after the ion-exchange reaction of MMT with the cationic complexes, respectively (Fig. 5). An increase in the interlayer distance, leads to a shift of the diffraction peak toward lower angles and confirms that the intercalation reaction and surface modification of MMT are occurred. This means that the basic structures of the MMT are kept, the layers only propped open and the basal distances are increased

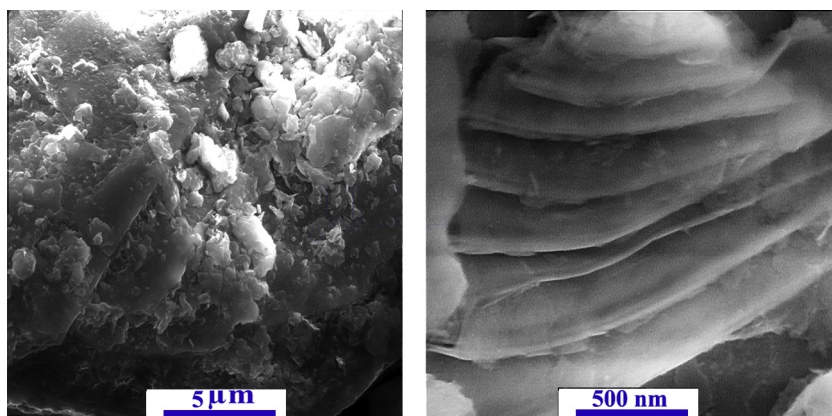


Fig. 6. The SEM.

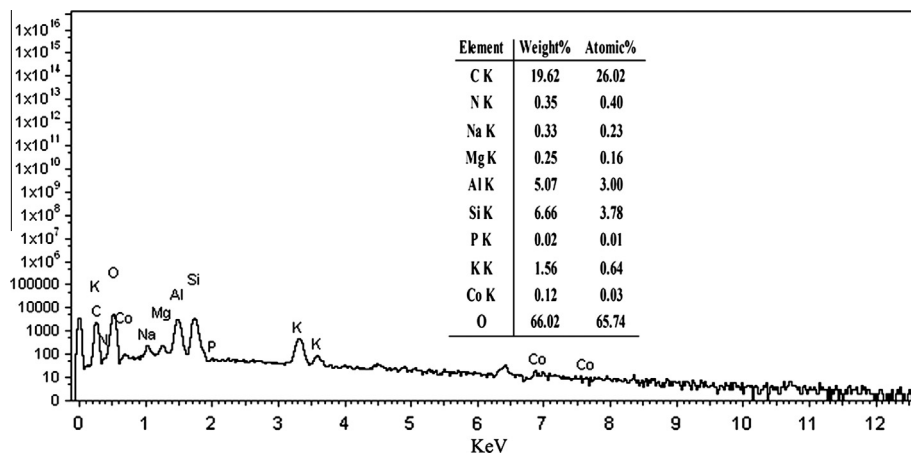


Fig. 7. The EDX of the MMT-PBu₃.

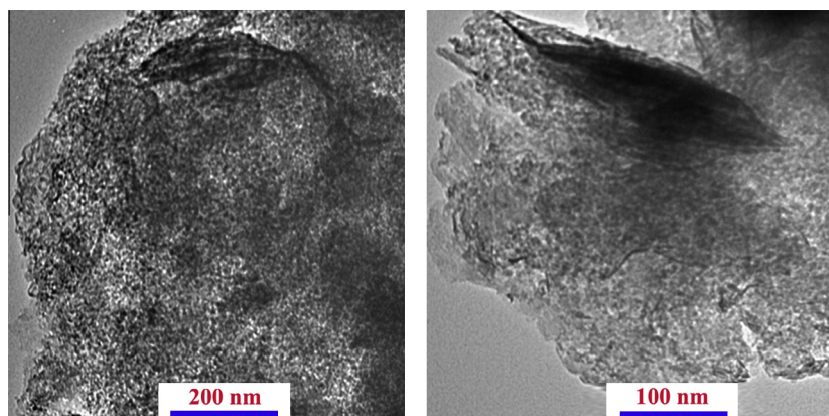


Fig. 8. The TEM images of the MMT-PBu₃.

significantly, providing evidence that the intercalation reaction has occurred successfully.

Morphology analysis

The SEM images of the MMT-PBu₃ were studied by SEM technique (Fig. 6). According to the SEM images, the MMT-PBu₃ has a layer structure. Further information was obtained using EDX. Fig. 7 shows the EDX spectrum of the MMT-PBu₃ particle. In the EDX spectrum, ten elements can be observed, i.e. carbon (C), oxygen (O), magnesium (Mg), aluminum (Al), silicon (Si), potassium (K), sodium (Na), phosphorus (P), nitrogen (N), and cobalt (Co). The high percent of the carbon observed in the EDX is associated with the coating materials sputtered on the sample. The presence of Co, P and N in the EDX confirms the presence of the Schiff base complex in the interlayer of the MMT. All remaining elements represent components of the MMT. Also the absence of fluorine in the EDX spectrum provided that the intercalation reaction has occurred successfully.

TEM images of MMT-PBu₃ nanohybrid are given in Fig. 8. According to the TEM images the thickness of the silicate layers of the organoclay is about 2–5 nm and no aggregation was observed in the TEM images of the MMT-PBu₃. The spaces between silicate layers are around 2 nm. Therefore, these TEM micrographs confirmed the results obtained by XRD in the form of small peaks.

Thermal degradation characteristics

The TGA and DTG curves of MMT, MMT-PPh₃ and MMT-PBu₃ are shown in Figs. 9 and 10. The thermal analysis of clay shows

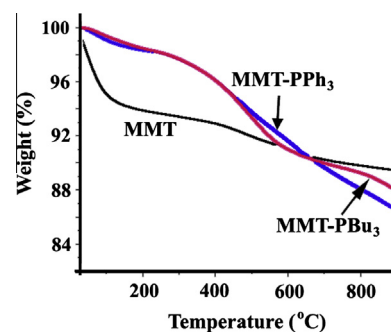


Fig. 9. The TGA thermogram of the hybrid materials.

that the main weight losses (5.9%) occur at the temperature of 30–270 °C, which can be attributed to the loss of physically adsorbed water. Second mass losses (1.9%) occur at the temperature range of 270–540 °C, correspond to the loss of water which is bonded to the clay layers. Last weight losses (2.2%), is due to the loss of hydroxyl groups of clay. Decomposition of MMT-PPh₃ and MMT-PBu₃ compounds occur in three steps, the mass loss (1.7%) at the room temperature to 210 °C is due to the adsorbed water. Second decomposition step (5.8%), in MMT-PPh₃ starts at 210 °C and ended at 560 °C is according to decomposition of Schiff base complex [43–47] which intercalated to the clay layers. In MMT-PBu₃ the second step shows 8.7% weight loss at the temperature of 220–750 °C. The weight loss in the third step is 5.97% and 1.70% for MMT-PPh₃ and MMT-PBu₃, respectively.

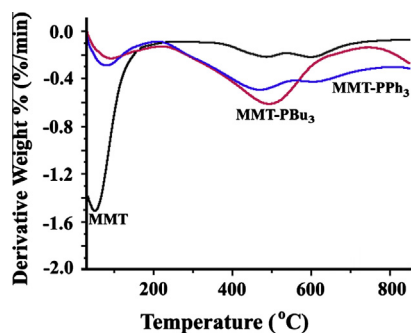


Fig. 10. The DTG thermogram of the hybrid materials.

The residue for MMT-PBu₃ and MMT-PPh₃ is about 88% and 87.5%, respectively.

Conclusions

In summary in this investigation at first, [Co(Me₂Salen)(PBu₃)(OH₂)]BF₄ and [Co(Me₂Salen)-(PPh₃)(Sol_v)]BF₄ complexes were synthesized and the structure of these compounds was confirmed by different techniques. The FT-IR and ¹H NMR and X-ray crystallography confirmed that the synthesized complexes contain Schiff base, phosphine and counter ion. The X-ray crystallography results show that the synthesized complexes are hexacoordinated in the solid state. Then nanohybrid materials of the above complexes and MMT were prepared in ethanol solution via simple ion-exchange reaction. FT-IR, TGA/DTG, XRD, SEM, EDX and TEM techniques were used for characterization of these new materials. The XRD results of the MMT-PR₃ show that the Schiff base complexes are intercalated in the interlayer spaces of MMT. According to the SEM and TEM micrographs the resulting hybrid nanomaterials have layer structures. TGA/DTG results show that the intercalation reaction has occurred successfully.

Acknowledgements

We wish to express our gratitude to the Research Affairs Division Isfahan University of Technology (IUT), Isfahan, for partial financial support. Further financial support from National Elite Foundation (NEF), Iran Nanotechnology Initiative Council (INIC) and Center of Excellency in Sensors and Green Chemistry Research (IUT) is gratefully acknowledged.

Appendix A. Supplementary materials

CCDC No. 965297 contains the supplementary crystallographic data for [Co(Me₂Salen)(PPh₃(OH₂)]BF₄, respectively. These data can be obtained at www.ccdc.cam.ac.uk/deposit {or from the Cambridge Crystallographic Data Center 12, Union Road Cambridge CB2 1EZ, UK; Fax: (internet) +44-1223/336-033; E. mail: deposit@ccdc.cam.ac.uk}. Supplementary data associated with this article can be found, in the online version, at <http://dx.doi.org/10.1016/j.saa.2014.02.089>.

References

- [1] K. Minagawa, M.R. Berber, I.H. Hafez, T. Mori, M.T. Tanaka, *J. Mater. Sci.: Mater. Med.* 23 (2012) 973–981.
- [2] X. Miao, T. Wang, F. Chai, X. Zhang, C. Wang, W. Sun, *Nanoscale* 3 (2011) 1189–1194.
- [3] E. Ruiz-Hitzky, A. Van Meerbeeck, in: F. Theng, B.K.G. Lagaly (Eds.), *Handbook of Clay Science*, Bergaya, Elsevier, Amsterdam, 2006.
- [4] Z. Zhao, T. Tang, Y. Qin, B. Huang, *Langmuir* 19 (2003) 9260–9265.
- [5] R.R. Tiwari, K.C. Khilar, U. Natarajan, *Appl. Clay Sci.* 38 (2008) 203–208.
- [6] D.R. Katti, P. Ghosh, S. Schmidt, K.S. Katti, *Biomacromolecules* 6 (2005) 3276–3282.
- [7] S. Mallakpour, M. Dinari, *Appl. Clay Sci.* 51 (2011) 353–359.
- [8] S. Ramesh, A. Sivasamy, M. Alagar, F. Chandrasekar, *J. Compos. Mater.* 45 (2011) 1483–1489.
- [9] S. Mallakpour, M. Dinari, H. Hadadzadeh, *J. Incl. Phenom. Macrocy. Chem.* 7 (2013) 463–470.
- [10] Z. Sun, Y. Park, S. Zheng, G.A. Ayoko, R.L. Frost, *J. Colloid Interf. Sci.* 408 (2013) 75–81.
- [11] S.M. Polson, R. Cini, C. Pifferi, L.G. Marzilli, *Inorg. Chem.* 36 (1997) 314–322.
- [12] E.C. Niederhoffer, J.H. Timmons, A.E. Martell, *Chem. Rev.* 84 (1984) 137–203.
- [13] K. Matsuura, S. Maeda, Y. Araki, Y. Ishido, T. Murai, *Tetrahedron* 33 (1977) 2869–2872.
- [14] A. Nishinaga, T. Tsutsui, S. Yamazaki, T. Matsuura, *Tetrahedron Lett.* 29 (1988) 4115–4118.
- [15] B. Golles, B. Speiser, H. Stahl, J. Sieglén, J. Strahle, *Z. Naturforsch.* 51b (1996) 388–392.
- [16] M. Asadi, A.H. Sarvestani, *Can. J. Chem.* 79 (2001) 1360–1365.
- [17] M. Asadi, A.H. Sarvestani, B. Hemateenejad, *J. Chem. Res.* (2002) 520–523.
- [18] A.H. Sarvestani, A. Salimi, S. Mohebbi, R. Hallaj, *J. Chem. Res.* (2005) 190–193.
- [19] A.H. Sarvestani, S. Mohebbi, *J. Chem. Res.* (2006) 257–260.
- [20] A.H. Kianfar, S. Zargari, *J. Coord. Chem.* 61 (2008) 341–352.
- [21] M. Asadi, M.B. Ahmadi, Kh. Mohammadi, Z. Asadi, A.H. Sarvestani, *J. Chem. Thermodyn.* 36 (2004) 141–146.
- [22] M. Asadi, A.H. Kianfar, S. Torabi, K. Mohammadi, *J. Chem. Thermodyn.* 40 (2008) 523–528.
- [23] A.H. Sarvestani, M. Asadi, M. Abbasi, *J. Chem. Res.* 1 (2007) 56–59.
- [24] M. Asadi, A.H. Sarvestani, Z. Asadi, M. Setoodekhah, *Synth. React. Inorg., Met.-Org. Nano-Met.* 35 (2005) 639–644.
- [25] M. Asadi, M. Setoodekhah, A.H. Kianfar, *J. Iran. Chem. Soc.* 7 (2010) 38–44.
- [26] J. Kjeld, C. van Bommel, W. Verboom, H. Kooijman, A.L. Spek, N.D. Reinhoudt, *Inorg. Chem.* 37 (1998) 4197–4203.
- [27] G.M. Sheldrick, SHELX97, Program for Crystal Structure Solution, University of Göttingen, Germany, 1997.
- [28] G.M. Sheldrick, *Acta Cryst.* A64 (2008) 112–122.
- [29] A.J.C. Wilson (Ed.), *International Tables For X-ray Crystallography*, Vol. C, Kluwer Academic Publisher, Dordrecht, The Netherlands, 1995.
- [30] Bruker, SADABS, Bruker AXS Inc., Madison, Wisconsin, USA, 2005.
- [31] A.H. Kianfar, V. Sobhani, M. Dostani, M. Shamsipur, M. Roushani, *Inorg. Chim. Acta* 355 (2011) 108–112.
- [32] G. Tazher, G. Mestroni, A. Puxeddu, R. Costanzo, G. Costa, *J. Chem. Soc.* (1971) 2504–2507.
- [33] N.S. Biradar, V.H. Kulkarni, *J. Inorg. Nucl. Chem.* 8 (1971) 2451–2457.
- [34] N.S. Biradar, G.V. Karajagi, T.M. Aminabhavi, *Inorg. Chim. Acta* 82 (1984) 211–214.
- [35] J.A. Bertrand, P.G. Eller, *Inorg. Chem.* 4 (1974) 927–934.
- [36] E. Ochiai, K. Long, C.R. Sperati, D.H. Busch, *J. Am. Chem. Soc.* 91 (1969) 3201–3206.
- [37] D.F. Shriver, P.W. Atkins, in: *Inorganic Chemistry*, Oxford University Press, 1999, p. 240.
- [38] Y.L. Zhang, W.J. Ruan, X.J. Zhao, H.G. Wang, Z.A. Zhu, *Polyhedron* 22 (2003) 1535–1545.
- [39] J. Welby, L.N. Rusere, J.M. Tanski, L.A. Tyler, *Inorg. Chim. Acta* 362 (2009) 1405–1411.
- [40] H. Chen, D. Han, T. Li, H. Yan, W. Tang, *Inorg. Chem.* 35 (1996) 1502–1508.
- [41] M. Amirnasr, R. Vafazadeh, A.H. Mahmoudkhani, *Can. J. Chem.* 80 (2002) 1196–1203.
- [42] T.L. Brown, K.J. Lee, *Coord. Chem. Rev.* 128 (1993) 89–116.
- [43] A.H. Kianfar, L. Keramat, M. Dostani, M. Shamsipur, M. Roushani, F. Nikpour, *Spectrochem. Acta* 77 (2010) 424–429.
- [44] A.H. Kianfar, M. Dostani, *Spectrochem. Acta* 82 (2011) 69–73.
- [45] A.H. Kianfar, M. Bahramian, H. Khavasi, *Spectrochem. Acta* 94 (2012) 302–307.
- [46] A.H. Kianfar, M. Paliz, M. Roushani, M. Shamsipur, *Spectrochem. Acta* 82 (2011) 44–48.
- [47] A.H. Kianfar, S. Ramazani, R. Hashemi Fath, M. Roushani, *Spectrochem. Acta* 105 (2013) 374–382.